CHEMICAL ENGINEERING TRANSACTIONS
VOL. 62, 2017

A publication of AIDIC
The Italian Association of Chemical Engineering
Online at www.aidic.it/cet

Guest Editors: Fei Song, Haibo Wang, Fang He

ISBN 978-88-95608- 60-0; **ISSN** 2283-9216

DOI: 10.3303/CET1762011

Grinding Characteristics of Molybdenum Tailings and Properties of Composite Mortar Containing Molybdenum Tailings

Jun Li[a], Ning Chang[a], Shichang Liu[b], Changlong Wang[c,a,d*], Shenhua Jiao[e]

[a]School of Civil Engineering, Hebei University of Engineering, Handan 056038, China
[b]Shandong Longquan Pipeline Engineering Co., Ltd, Zibo 255200, China
[c]Jiangxi Key Laboratory of Mining Engineering, Jiangxi University of Science and Technology, Ganzhou 341000, China
[d]Tianjin Sunenergy Sega Environmental Science & Technology Co. Ltd, Tianjin 300000, China
[e]China Ordnance Industry Survey and Geotechinical Institute, Beijing 100053, China
13716996653@139.com

In order to promote the application of molybdenum (Mo) tailings in concrete industry, this paper studies the grinding characteristics of Mo tailings, the mechanical and hydration properties of mortars containing Mo tailings by X-ray diffraction (XRD), scanning electron microscope (SEM), laser particle size analysis, specific surface area analysis and strength test. The optimal grinding time is 80 mins to obtain the ground Mo tailings (-0.16 mm) with a specific surface area of 501 m^2 kg^{-1} as mineral admixtures to the cementitious materials. With the coarse Mo tailings (+0.16 mm) as fine aggregate, composite mortars with a good workability were obtained with the compressive strength of 83.5 MPa and the flexural strength of 14.4 MPa after cured for 28 days. The comprehensive utilization rate of Mo tailings is 71 % in the composite mortars. The hydration of the cementitious composite containing Mo tailings at early age is primarily due to the hydration of the cement clinker (CC). While the large amount of quartz remains inert, the pozzolanic reaction of ground Mo tailings leads to the strength increases in long term. The main hydration phases in the cementitious composite are calcium silicate hydrates (C-S-H gels) and ettringite (AFt).

1. Introduction

According to the statistics, there were 14.6 billion tons of tailings in China, which include ferrous metal ore tailings are and non-ferrous metal ore tailings. The amount of non-ferrous metal tailings is 2.2 billion tons by far with an increase rate of 140 million tons per year. The storage of ore tailings is a large potential threat to the ecosystem and society, while it also limits the sustainability of mining economy (Wang et al., 2016). Comprehensive recycling and utilization of industrial solid waste is one of the important measures for industrial sustainable development. As the technology advances, ore tailings are considered to be a potential resources and its recycling is drawing more and more attention of the public (Ghose and Sen, 2001). It is thought that utilizing of the waste solid may not only solve the shortage of raw materials in industrial production, but also eliminated the environmental pollutions and ecological destruction potentially caused by discarding hazardous waste at dump sites in the future. The tailings are mainly used as filling materials with a utilization rate more than 50% (Cao and Song, 2017; Deng et al., 2017), while other applications include valuable metals recovery (Luo et al., 2017; Lei et al., 2017), preparation of building materials (a utilization rate more than 40%) (Zhao et al., 2012), trace element fertilizer, and soil conditioner (Reid et al., 2009). As the investment of infrastructure construction keeps increasing in China, the increasing demand for innovative construction materials provides a promising future for the utilization of tailings. However, there are few studies in the utilization of non-ferrous metal tailings. As a new type of high technology concrete, high performance concrete (HPC) represents the future of concrete technology, its durability has obtained a dramatic improvement compared to traditional concrete, which shows that concrete has marched towards high technology materials (Zhao et al., 2015; Wu et al., 2017). Mineral admixtures have become the sixth essential component for high tech concrete, in which fly ash is the most widely used mineral admixtures. Fly ash can reduce bleeding of fresh concrete, lower the

Please cite this article as: Jun Li, Ning Chang, Shichang Liu, Changlong Wang, Shenhua Jiao, 2017, Grinding characteristics of molybdenum tailings and properties of composite mortar containing molybdenum tailings, Chemical Engineering Transactions, 62, 61-66
DOI:10.3303/CET1762011

hydration heat, improve the durability of concrete and improve the long term strength of concrete (Upadhyaya et al., 2015). Based on the principle of active powder concrete, this paper studies the feasibility of high strength structural components containing molybdenum (Mo) tailings as the main raw materials, along with ground blast furnace slag (GBFS), cement clinker (CC), and gypsum of flue gas desulfurization waste (FGDW). The grinding characteristics of Mo tailings and the mechanical and hydration properties of the composite mortars containing Mo tailings are analyzed using X-ray diffraction (XRD), scanning electron microscope (SEM), laser particle size analysis, specific surface area (SSA) analysis and strength test.

2. Materials and Experimental methods

2.1 Materials

The mortar is prepared using the following raw materials: molybdenum (Mo) tailings, ground blast furnace slag (GBFS), cement clinker (CC), gypsum of flue gas desulfurization waste (FGDW) and water reducer (WC). The chemical compositions of the raw materials are listed in Table 1.
Mo tailings. It is provided by Jiulong Mining LLC., Luonan, Shaanxi Province, China. The chemical composition of the Mo tailings is listed in Table 1. The tailings is high silica tailings with the SiO_2 content of 73% by mass, which is mainly in the form of inert quartz. Fig. 1 shows the XRD pattern of the tailings. It indicates that it includes quartz (SiO_2) as the main mineral phase, and phlogopite ($Al_2K_2O_6Si$), feldspar ($CaO{\cdot}Al_2O_3{\cdot}2SiO_2$) and hornblende ($(Ca\ Na)_2(Mg, Fe, Al)_5(Si, Al)_8O_{22}(OH, F, Cl)_2$) as minor phases. Table 2 lists its particle size distribution. The percentage of particles with a size smaller than 0.16 mm and 0.08 mm is 29.91 % and 14.65 %, respectively. 64.01 % of particles are with the size range of 0.16 mm-0.63 mm, which indicates that this Mo tailings belongs to extremely fine tailings.

Table 1: Chemical composition of raw materials (% by mass)

Materials	SiO_2	CaO	Al_2O_3	Fe_2O_3	FeO	MgO	K_2O	Na_2O	SO_3	LOI
Mo tailings	73.04	4.01	5.27	5.33	3.54	2.26	2.12	0.24	-	2.45
GBFS	34.90	35.46	14.65	0.70	-	10.52	0.35	0.27	-	0.38
CC	22.50	66.30	4.86	3.43	-	0.83	-	-	0.31	-
FGDW	3.14	45.31	1.48	0.71	-	0.58	0.35	0.11	47.26	-

Table 2: Sieve analysis of Mo tailings

Size grade/mm	Percentage/%	Cumulative percentage/%
+2.5	0.07	99.85
-2.5+1.25	0.31	99.78
-1.25+0.63	5.55	99.47
-0.63+0.315	26.68	93.92
-0.315+0.16	37.33	67.24
-0.16+0.08	15.26	29.91
-0.08	14.65	14.65
Total	100	

GBFS. Table 1 shows its chemical composition. The SiO_2 and CaO combined amount of GBFS in Table 1 is above 50 % by mass, which exists mainly as gehlenite ($Ca_2Al(AlSi)O_7$).
CC. It is from Jidong Cement LLC., Tangshan, Hebei Province, China, with the chemical composition listed in Table 1.
FGDW. The primary mineral phase of FGDW is $CaSO_4{\cdot}2H_2O$. The specific surface area of the FGDW is 280 $m^2\ kg^{-1}$. Its chemical compositions are listed in Table 1, and 0.08 mm sieve residual is less than 7.9 %.
WC. It is polycarboxylic superplasticizer from Muhu Chemical Admixture LLC., Beijing, China.

2.2 Experimental methods

2.2.1 Preparation of cementitious composites

The sieved MO tailing (with the particle size smaller than 0.16 mm and the water content less than 0.1 wt. %) was grinded for 40, 60, 80 and 100 mins by a ball mill (SMΦ500 mm×500 mm). The different ground MO tailings was mixed with ground CC, GBFS, FGDW based on the proportions of the cementitious composites in Table 3. The SSA of each component is listed in Table 4.

Table 3: Mixture composition of cementitious composites (% by mass)

Group	MO tailings	CC	GBFS	FGDW	SSA of Mo tailings/ (m^2 kg^{-1})
A-1	42	17	33	8	389
A-2	42	17	33	8	443
A-3	42	17	33	8	501
A-4	42	17	33	8	652

Table 4: Specific surface area of grinding materials

Component	MO tailings				GBFS	CC	FGDW
	40/min	60/min	80/min	100/min			
SSA/ (m^2 kg^{-1})	389	443	501	652	568	483	450

2.2.2 Preparation of composite mortars

As the fine aggregate, coarse MO tailings (+0.16 mm) was mixed with the above cementitious composites as a mass ratio of 1:1. The dosage of WC was 0.4 wt. % of cementitious composites. The water to cementitious composite ratio was 0.23. The mixed fresh mortar was cast into the molds with the dimension of 40 mm×40 mm×160 mm, which were cured in moist room (RH>90%, 20±1 ºC) for 1 days. Then the demolded specimens were cured in lime water at 20±1 ºC until the specific ages (3, 7, and 28 days). The compressive and flexural strength of specimens was measured at varying ages.

2.2.3 Property characterizations

MO tailings were sieved using ZBSX-92A top-hit standard shaker. According to the Chinese National Standard GB/T 19077.1-2008 *Particle size analysis - Laser diffraction methods - Part 1: General principles*, the particle size distribution of ground Mo tailings was analyzed using laser particle size analyzer (MASTER SIZER 2000, the analysis range was 0.02~2000.00 μm) with ethanol as the dispersant. SSA of Mo tailings was measured using dynamic specific surface area analyzer (SSA-3200). The fluidity of the fresh mortar was measured using the Chinese standard GB/T2419-205. The compressive strength test of mortars was based on the Chinese National Standard GB/T 17671-1999 *Method of testing cement-determination of strength*. The strength was measured using hydraulic pressure testing machine (YES-300) with a maximum load of 300 KN and a loading rate of 2.0±0.5 kN/s. The XRD spectras were obtained using a D/Max-RC diffractometer (Japan) with Cu-Kα radiation, voltage of 40 kV, current of 150 mA and 2θ scanning ranging between 5 ° and 85 °. And the wavelength is 1.5406 nm. FE-SEM observation was performed to analyse the mineral phase and the hydration products of the paste samples using a Zeiss SUPRA^{TM}55 scanning electron microscope coupled with a Be4-U92 energy spectrum.

3. Results and discussion

3.1 The influence of grinding time on the mechanical properties of composite mortars containing MO tailings

The mechanical properties and workability of mortar composites containing MO tailings after varying grinding time were measured, which can help to determine the optimal grinding time. Table 5 shows the mechanical properties and fluidity of varying mortars. After 80 mins grinding, the SSA of MO tailings is 501 m^2 kg^{-1}, and the corresponding mortar (B-3) achieved the max compressive and flexural strength with values of 82.5 MPa and 14.7 MPa, respectively. Meanwhile, B-3 fresh mortar had a good fluidity, which complies the requirements of construction. The compressive strength and flexural strength of mortar increases first until a peak and then decreases as the grinding time increases.

Table 5: Test results of properties of specimens

Group	MO tailings grinding time/min	Fluidity /mm	Compressive strength/MPa			Flexural strength/MPa		
			3 d	7 d	28 d	3 d	7 d	28 d
B-0	0	134	20.1	27.2	33.7	0	0	0.5
B-1	40	167	38.2	43.6	58.7	3.2	5.5	6.9
B-2	60	185	46.8	56.0	71.4	3.7	7.0	10.2
B-3	80	189	55.2	71.6	83.5	4.7	8.8	14.7
B-4	100	210	53.1	67.5	77.9	4.5	9.0	11.9

The fluidity keeps increasing as the grinding time increases. The B-0 mortar with original MO tailings has the lowest strength, which cannot meet the requirement of the high strength structural elements. This indicates that the original MO tailings has little reactivity, which is inappropriate to be used as mineral admixture. The MO tailings herein contains a large amount of silica in the form of quartz (in Table 1). After ball milling, a portion of crystallized SiO_2 is converted to active SiO_2 with a pozzolanic activity, which may be able to react during hydration as a supplementary cementitious material in the high strength mortar.

3.2 Microstructure analysis of ground MO tailings

3.2.1 XRD

Figure 1 shows the XRD patterns of MO tailings after different grinding time. Quartz is the main mineral phases in all the MO tailings, regardless of the grinding time. However, the peak intensity of the mineral phases decreases as the grinding time increases. This is due to the reduction in the degree of crystallization of the minerals in the MO tailings, which results in the formation of amorphous components. At first, mechanical ball milling dramatically decreases the particle sizes of the tailings, which increases its SSA. As the time of mechanical grinding, the chemical bonds in the mineral crystals were partially broken, and this introduces the structural change and dehydration of the crystals and potentially the formation of new phases. The semi-quantitative analysis of XRD patterns in Figure 1 shows a content of silicate minerals above 70 %. One portion of inert silicate minerals was activated to turn to active silicate by the mechanical activation.

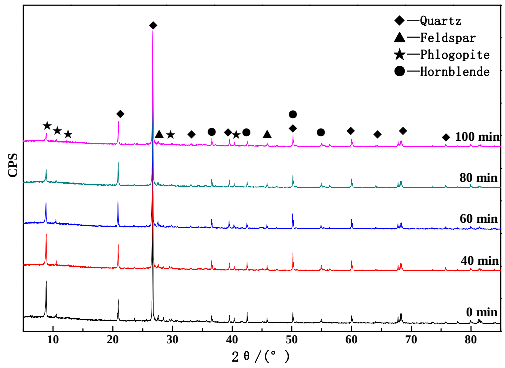

Figure 1: XRD patterns of MO tailings.

3.2.2 Particle size distribution and SEM analysis

Figure 2(a) and (b) show the particle size distribution (PSD) and accumulative distribution of MO tailings after different grinding time. As the grinding time increases, the peak particle size decreases towards 10 μm. The peak particle size was below 10 μm in MO tailings after 100 mins grinding. After the grinding, the dramatic reduction in the particle size and increase in SSA were observed. It should be noted that the bi-modal feature in the PSD of MO tailings after 100 mins, which indicates the sub-micro agglomeration of particles below 100 μm. One hypothesis may be that new phases were created due to the broken chemical bonds in the minerals. Another hypothesis may be the strong electrostatic interaction in the sub-micro particles. The hypothesized agglomeration may result in the strength increase in the mortar with MO tailings after 100 mins, compared to that of 80 mins.

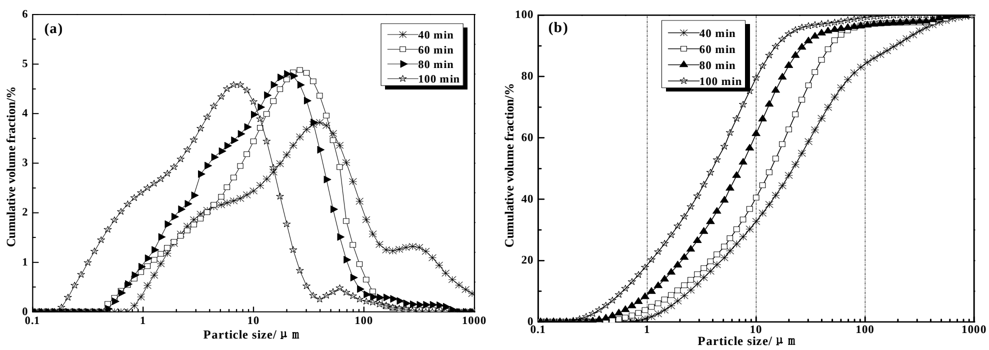

Figure 2: Particle size distributions of MO tailings after different grinding time: (a)- particle size distribution (PSD); (b)-accumulative distribution.

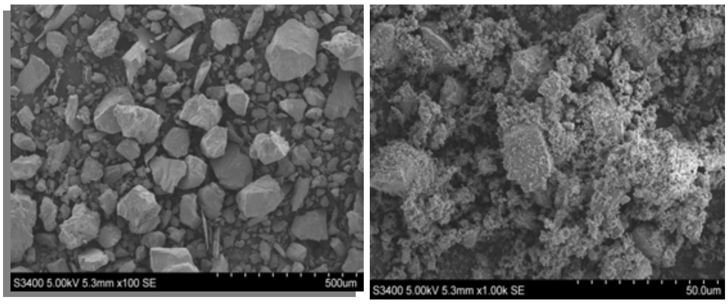

Figure 3: SEM images of Mo tailings and grinding 80 mins.

Figure 3 show the SEM images of original MO tailings and the one after 80 mins grinding. Figure 3(a) clearly shows the irregular shapes of the coarse tailing particles after mineral processing. Coarse particles are surrounded by fine particles, which increases the water demand in the system and influences the long term strength. Figure 3(b) indicates the round fine particles in the grinded MO tailings. The particles after grinding are mainly sub-micrometer and nanometer level, which indicates its filler effect. The refined graded MO tailings helps increase the strength and workability of the cementitious composites. It also helps decrease the hydration heat. Thus, 80 mins are the optimal grinding time, and the optimal SSA of MO tailings is about 500 $m^2\,kg^{-1}$.

3.3 Analysis of hydration products

3.3.1. XRD

Figure 4 shows the XRD patterns of A-3 cementitious composite with a w/b of 0.19 at varying ages of 3 d, 7 d and 28 d. High intensity peaks of quartz were obtained, which indicates that quartz did not participate in hydration. At Day 3, C-S-H gels and $Ca(OH)_2$ were observed due to the hydration of C_3S ($3CaO{\cdot}SiO_2$) and C_2S ($2CaO{\cdot}SiO_2$) in the CC; ettringite (AFt, $3CaO{\cdot}Al_2O_3{\cdot}3CaSO_4{\cdot}32H_2O$) was observed as well due to the reaction between C_3A ($3CaO{\cdot}Al_2O_3$) and FGDW. As hydration continues, more C-S-H gels and AFt formed in the paste at Day 28. This may be partially due to the active SiO_2 and Al_2O_3 in the chemical admixtures reacted with $Ca(OH)_2$. This helps densify the microstructure of the composites and increase the strength.

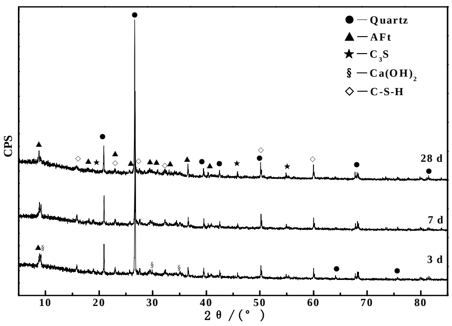

Figure 4: XRD patterns of the A-3 cementitious composite at varying ages.

3.3.2 SEM Images

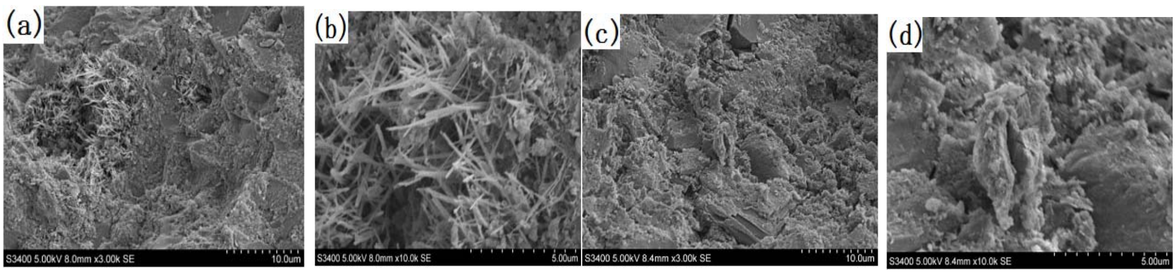

Figure 5: SEM images of hardened test block in different age.

Figure 5 shows the SEM images of B-3 mortar at varying ages of 3 d, 7 d, and 28 d. Figure 5(a) indicates the formation of needle-shaped AFt and C-S-H gels at the early age of 3 days. Figure 5(b) is the 1000x image at

Day 3. It shows the inter-connection of the needle-shaped crystals as hydration continues, which helps increase the strength while there still remains a lot of unreacted particles. Figure 5(c) and 5(d) are the SEM images of hardened mortar at Day 28. It shows that a lot of AFt needle-shaped crystals are surrounded by C-S-H gels, which indicates a high degree of hydration. And Figure 6(d) shows the intensified microstructure with voids being filled by hydration products. It leads to the increased strength in long term.

4. Conclusions

(1) The optimal grinding time for MO tailings in this paper was 80 mins. The corresponding mortar, which has a waste utilization rate of 71.5 %, achieved the compressive strength flexural strength of 83.5 MPa and 14.7 MPa with a good workability.
(2) The ground MO tailings have pozzolanic reactivity by mechanical activation during grinding. Mechanical activation mainly lie in the finer particle sizes, reduction in crystallization degree, formation of amorphous phases and the increase in chemical energy. However, over-grinding may introduce the agglomeration of particles.
(3) Based on the observations in XRD and SEM results of hardened composites, the main hydration products include C-S-H gels and AFt, which results in the increase of the strength.

Acknowledgments

The authors gratefully acknowledge financial support from China Postdoctoral Science Foundation (2016M602082), supported by Science and Technology Research Project of Higher Education Universities in Hebei Province (ZD2016014, QN2016115), supported by Construction Science and Technology Foundation of Hebei Province (2012-136), supported by Handan Science and Technology Research and Development Plan Program (1621211040-3), supported by Jiangxi Postdoctoral Daily Fund Project (2016RC30).

Reference

Cao S., Song W.D., 2017, Effect of filling interval time on the mechanical strength and ultrasonic properties of cemented coarse tailing backfill, International Journal of Mineral Processing, 166, 62-68, DOI: 10.1016/j.minpro.2017.07.005.

Deng D.Q., Liu L., Yao Z.L., Song K.I.-I.L., Lao D.Z., 2017, A practice of ultra-fine tailings disposal as filling material in a gold mine, Journal of Environmental Management, 196, 100-109, DOI: 10.1016/j.jenvman.2017.02.056.

Ghose M.K., Sen P.K., 2001, Characteristics of iron ore tailing slime in India and its test for required pond size, Environmental Monitoring and Assessment, 68(1), 51–61, DOI: 10.1023/A:1010782822753.

Lei C., Yan B., Chen T., Xiao X.M., 2017, Recovery of metals from the roasted lead-zinc tailings by magnetizing roasting followed by magnetic separation, Journal of Cleaner Production, 158, 73-80, DOI: 10.1016/j.jclepro.2017.04.164.

Luo M.J., Liu C.L., Jiang Y.F., Xue J., Li P., Yu J.G., 2017, Green recovery of potassium and aluminum elements from alunite tailings using gradient leaching process, Journal of Cleaner Production, 168, 1080-1090, DOI: 10.1016/j.jclepro.2017.09.090.

Reid C., Bécaert V., Aubertin M., Rosenbaum R.K., Deschênes L., 2009, Life cycle assessment of mine tailings management in Canada, Journal Cleaner Production, 17, 471-479, DOI: 10.1016/j.jclepro.2008.08.014.

Upadhyaya S., Goulias D., Obla K., 2015, Maturity-based field strength predictions of sustainable concrete using high-volume fly ash as supplementary cementitious material, Journal of Materials in Civil Engineering, 27(5), 69-75, DOI: 10.1061/(ASCE)MT.1943-5533.0001123.

Wang C.L., Ni W., Zhang S.Q., Wang S., Gai G.S., Wang W.K., 2016, Preparation and properties of autoclaved aerated concrete using coal gangue and iron ore tailings, Construction and Building Materials, 104, 109-115, DOI: 10.1016/j.conbuildmat.2015.12.041.

Wu Z.M, Khayat K.H., Shi C.J., 2017, Effect of nano-SiO_2 particles and curing time on development of fiber-matrix bond properties and microstructure of ultra-high strength concrete, Cement and Concrete Research, 95, 247-256, DOI: 10.1016/j.cemconres.2017.02.031.

Zhao H., Sun W., Wu X.M., Gao B., 2015, The properties of the self-compacting concrete with fly ash and ground granulated blast furnace slag mineral admixtures, Journal of Cleaner Production, 95, 66-74, DOI: 10.1016/j.jclepro.2015.02.050.

Zhao S.J., Fan J.J., Sun W., 2014, Utilization of iron ore tailings as fine aggregate in ultra-high performance concrete, Construction and Building Materials, 50, 540-548, DOI: 10.1016/j.conbuildmat.2013.10.019.